Journal of Sound and Vibration (2001) **239**(5), 1013–1036
doi:10.1006/jsvi.2000.3182, available online at http://www.idealibrary.com on IDEAL®

GLOBAL AND CHAOTIC DYNAMICS FOR A PARAMETRICALLY EXCITED THIN PLATE

W. ZHANG

College of Mechanical Engineering, Beijing Polytechnic University, Beijing 100022, *People's Republic of China. E-mail*: *sandyzhang0@yahoo.com*

(*Received* 15 *December* 1999, *and in final form* 12 *June* 2000)

The global bifurcations and chaotic dynamics of a parametrically excited, simply supported rectangular thin plate are analyzed. The formulas of the thin plate are derived by von Karman-type equation and Galerkin's approach. The method of multiple scales is used to obtain the averaged equations. Based on the averaged equations, theory of normal form is used to give the explicit expressions of normal form associated with a double zero and a pair of pure imaginary eigenvalues by Maple program. On the basis of the normal form, global bifurcation analysis of the parametrically excited rectangular thin plate is given by a global perturbation method developed by Kovacic and Wiggins. The chaotic motion of thin plate is found by numerical simulation.

1. INTRODUCTION

With the use of the thin plate in the large-space station and the cover skin for wings used in the shutter and modern aircraft, non-linear dynamics, bifurcations and chaos of thin plates are gaining more importance. For the studies on non-linear oscillations of thin plates in the case of large deformation, the researchers in the engineering have given a wide attention. In the past decade, the researchers have conducted a number of studies on non-linear oscillations, bifurcations and chaos of thin plates and thin shallow arch structures. Holmes [1] studied flow-induced oscillations and bifurcations of thin plate and simplified this problem to two-degree-of-freedom (d.o.f.) non-linear system and used center manifolds, theory of normal forms to study the degenerate bifurcations. Yang and Sethna [2] used the averaging method to study the local and global bifurcations in parametrically excited nearly square plate. From van Karman equation, they simplified this system to a parametrically excited two-d.o.f. non-linear oscillators with $Z_2 \oplus Z_2$-symmetry and analyzed the global behavior of averaged equations. The results obtained in reference [2] indicated that the heteroclinic loops exist and Smale horse and chaotic motions can occur. Based on the studies in reference [2], Feng and Sethna [3] made use of a global perturbation method developed by Kovacic and Wiggins [4] to study further the global bifurcations and chaotic dynamics of thin plate under parametric excitation, and obtained the conditions in which Silnikov-type homoclinic orbits and chaos can occur.

Hadian and Nayfeh [5] used the method of multiple scales to analyze asymmetric responses of non-linear clamped circular plates subjected to harmonic excitations and considered the case of a combination-type internal resonance. Pai and Nayfeh [6] presented a general non-linear theory for the studies on dynamics of elastic composite plates undergoing moderate-rotation oscillations by considering the geometric non-linearities. Sassi and Ostiguy [7] investigated effects of initial geometric imperfections on the

0022-460X/01/051013 + 24 $35.00/0

interaction between forced and parametric oscillations for simply supported rectangular plates. Nayfeh and Vakakis [8] used the method of multiple scales to study the subharmonic travelling waves of thin, axisymmetric, geometrically non-linear circular plates and found the non-linear interactions of pairs of modes with coincident linearized natural frequencies. Chang *et al.* [9] investigated the bifurcations and chaos of a rectangular thin plate with 1 : 1 internal resonance. Tian *et al.* [10, 11] used the averaging method and Melnikov technique to study local, global bifurcations and chaos of a two-d.o.f. shallow arch subjected to simple harmonic excitation for cases of 1 : 2 and 1 : 1 internal resonance respectively. Abe *et al.* [12] used the method of multiple scales to analyze two-mode response of simply supported thin rectangular laminated plates subjected to a harmonic excitation. Popov *et al.* [13] investigated the interaction between different modes of shell oscillations and bifurcations under parametric excitation by using system models with four of the lowest modes. Malhotra and Namachchivaya [14, 15] investigated the global bifurcations and chaotic dynamics of the shallow arch structures under 1 : 1 and 1 : 2 internal resonance conditions respectively.

This paper is focused on the studies for the global bifurcations and chaotic dynamics of the simply supported at the four-edge rectangular thin plate subjected to in-plane excitation. The case of 1 : 1 internal resonance and primary parametric resonance is considered. First it is based on von Karman-type equation, the governing equations of the rectangular thin plate are derived and the equations of motion with two-d.o.f. under parametrical excitation can be obtained by using Galerkin's approach respectively. Then the method of multiple scales can be used to find the averaged equations of the original non-autonomous system. From the averaged equations, the theory of normal form is applied to obtain the explicit formulas of normal form associated with a double zero and a pair of pure imaginary eigenvalues with the aid of Maple program. A global perturbation method developed by Kovacic and Wiggins [4] is utilized to give the analysis for the global and chaotic dynamics of the rectangular thin plate. The global bifurcation analysis indicates that there exist the heteroclinic bifurcations and the Silnikov-type homoclinic orbit in the averaged equations. The results obtained in this paper also show that the chaotic motion can occur in a parametrically excited rectangular thin plate. The numerical simulations verify the analytical prediction.

2. FORMULATION

We consider the simply supported at the four-edge rectangular thin plate where the edge lengths are a and b and thickness is h respectively. The thin plate is subjected to its plane excitation. We establish a Cartesian co-ordinate system shown in Figure 1 such that

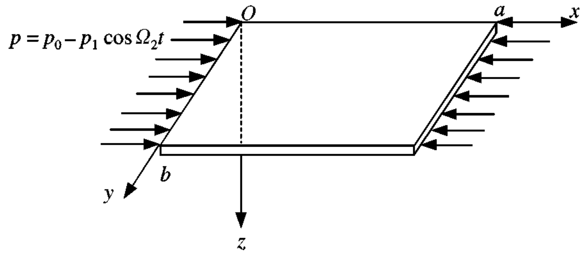

Figure 1. The model of a rectangular thin plate and the co-ordinate system.

co-ordinate Oxy is located in the middle surface of the thin plate. It is assumed that u, v and w represent the displacements of a point in the middle plane of the thin plate in the x, y and z directions respectively. The excitation in-plane of the thin plate may be expressed in the form $p = p_0 - p_1 \cos \Omega t$. From van Karman-type equations for the thin plate [16], we obtain the equations of motion for the rectangular thin plate as follows:

$$D\nabla^4 w + \rho h \frac{\partial^2 w}{\partial t^2} - \frac{\partial^2 w}{\partial x^2}\frac{\partial^2 \phi}{\partial y^2} - \frac{\partial^2 w}{\partial y^2}\frac{\partial^2 \phi}{\partial x^2} + 2\frac{\partial^2 w}{\partial x \partial y}\frac{\partial^2 \phi}{\partial x \partial y} + \mu \frac{\partial w}{\partial t} = 0, \tag{1}$$

$$\nabla^4 \phi = Eh\left[\left(\frac{\partial^2 w}{\partial x \partial y}\right)^2 - \frac{\partial^2 w}{\partial x^2}\frac{\partial^2 w}{\partial y^2}\right], \tag{2}$$

where ρ is the density of thin plate, $D = Eh^3/12(1 - v^2)$ is the bending rigidity, E is Young's modulus, v is the Possion ratio, ϕ is the stress function, and μ is the damping coefficient.

We assume that the simply supported boundary conditions can be written as

$$\text{at } x = 0 \text{ and } a, \quad w = \frac{\partial^2 w}{\partial x^2} = 0; \qquad \text{at } y = 0 \text{ and } b, \quad w = \frac{\partial^2 w}{\partial y^2} = 0. \tag{3}$$

The boundary conditions satisfied by the stress function ϕ may be expressed in following form:

$$u = \int_0^a \left[\frac{1}{E}\left(\frac{\partial^2 \phi}{\partial y^2} - v\frac{\partial^2 \phi}{\partial x^2}\right) - \frac{1}{2}\left(\frac{\partial w}{\partial x}\right)^2\right] \mathrm{d}x = \delta_x$$

and

$$h\int_0^b \frac{\partial^2 \phi}{\partial y^2}\,\mathrm{d}y = p \quad \text{at } x = 0 \quad \text{and} \quad a, \tag{4}$$

$$v = \int_0^b \left[\frac{1}{E}\left(\frac{\partial^2 \phi}{\partial x^2} - v\frac{\partial^2 \phi}{\partial y^2}\right) - \frac{1}{2}\left(\frac{\partial w}{\partial y}\right)^2\right] \mathrm{d}x = 0$$

and

$$\int_0^a \frac{\partial^2 \phi}{\partial x^2}\,\mathrm{d}x = 0 \quad \text{at } y = 0 \quad \text{and} \quad b, \tag{5}$$

where δ_x is the corresponding displacement in the x direction at the boundary.

We mainly consider the non-linear oscillations of thin plate in the first two modes. Thus, we write w in the form of

$$w(x, y, t) = u_1(t) \sin\frac{\pi x}{a} \sin\frac{3\pi y}{b} + u_2(t) \sin\frac{3\pi x}{a} \sin\frac{\pi y}{b}, \tag{6}$$

where $u_i(t)$ $(i = 1, 2)$ are the amplitudes of two modes respectively.

Substituting equation (6) into equation (2), considering the boundary conditions (4) and (5) and integrating, we may obtain the stress function as follows:

$$\begin{aligned}\phi(x,y,t) &= \phi_{20}(t)\cos\frac{2\pi x}{a} + \phi_{02}(t)\cos\frac{2\pi y}{b} + \phi_{60}(t)\cos\frac{6\pi x}{a}\\ &\quad + \phi_{06}(t)\cos\frac{6\pi y}{b} + \phi_{22}(t)\cos\frac{2\pi x}{a}\cos\frac{2\pi y}{b} + \phi_{24}(t)\cos\frac{2\pi x}{a}\cos\frac{4\pi y}{b}\\ &\quad + \phi_{42}(t)\cos\frac{4\pi x}{a}\cos\frac{2\pi y}{b} + \phi_{44}(t)\cos\frac{4\pi x}{a}\cos\frac{4\pi x}{b} - \frac{1}{2}py^2,\end{aligned} \tag{7}$$

where

$$\begin{aligned}&\phi_{20}(t) = \frac{9Eh}{32\lambda^2}u_1^2, \quad \phi_{02}(t) = \frac{9\lambda^2 Eh}{32}u_2^2, \quad \phi_{60}(t) = \frac{Eh}{288\lambda^2}u_2^2,\\ &\phi_{06}(t) = \frac{\lambda^2 Eh}{288}u_1^2, \quad \phi_{22}(t) = -\frac{\lambda^2 Eh}{(\lambda^2+1)^2}u_1u_2, \quad \phi_{24}(t) = \frac{25\lambda^2 Eh}{16(\lambda^2+4)^2}u_1u_2,\\ &\phi_{42}(t) = \frac{25\lambda^2 Eh}{16(4\lambda^2+1)^2}u_1u_2, \quad \phi_{44}(t) = -\frac{\lambda^2 Eh}{16(\lambda^2+1)^2}u_1u_2, \quad \lambda = \frac{b}{a}.\end{aligned} \tag{8}$$

In order to obtain the dimensionless equations, we introduce the transformations of variables and parameters

$$\begin{aligned}&\bar{x}_{\mathrm{i}} = \frac{(ab)^{1/2}}{h^2}u_{\mathrm{i}}, \quad (i=1,2), \quad \bar{p} = \frac{b^2}{\pi^2 D}p, \quad \bar{\Omega} = \frac{ab}{\pi^2}\left(\frac{\rho h}{D}\right)^{1/2}\Omega,\\ &\varepsilon = \frac{12(1-v^2)h^2}{ab}, \quad \bar{t} = \frac{\pi^2}{ab}\left(\frac{D}{\rho h}\right)^{1/2}t, \quad \bar{\mu} = \frac{a^2b^2}{\pi^2 h^4}\left(\frac{1}{12(1-v^2)\rho E}\right)^{1/2}\mu,\end{aligned} \tag{9}$$

where ε is a small parameter. For simplicity, we drop overbars in the following analysis. By means of Galerkin's method, substituting equations (6) and (7) into equation (1) and integrating, we obtain the equations of motion for the dimensionless as follows:

$$\begin{aligned}&\ddot{x}_1 + \varepsilon\mu\dot{x}_1 + (\omega_1^2 + 2\varepsilon f_1\cos\Omega t)x_1 + \varepsilon(\alpha_1 x_1^3 + \alpha_2 x_1 x_2^2) = 0,\\ &\ddot{x}_2 + \varepsilon\mu\dot{x}_2 + (\omega_2^2 + 2\varepsilon f_2\cos\Omega t)x_2 + \varepsilon(\beta_1 x_2^3 + \beta_2 x_1^2 x_2) = 0,\end{aligned} \tag{10}$$

where

$$\begin{aligned}&\alpha_1 = \frac{\lambda^2+81}{16\lambda^2}, \quad \beta_1 = \frac{1}{16}\left(81\lambda^2 + \frac{1}{\lambda^2}\right),\\ &\alpha_2 = \beta_2 = \frac{17\lambda^2}{(1+\lambda^2)^2} + \frac{625\lambda^2}{16(4+\lambda^2)^2} + \frac{625\lambda^2}{16(1+4\lambda^2)^2},\\ &\omega_k^2 = ((\omega_k^*)^2 - h_k p_0) \quad \text{and} \quad h_k = \begin{cases}1, & k=1,\\ 9, & k=2,\end{cases} \quad p_1^* = (\omega_1^*)^2 = \frac{(9+\lambda^2)^2}{\lambda^2},\\ &p_2^* = (\omega_2^*)^2 = \frac{(9\lambda^2+1)^2}{\lambda^2}, \quad f_k = \tfrac{1}{2}h_k p_1 \quad \text{and} \quad k = 1, 2,\end{aligned} \tag{11}$$

where $\omega_k (k = 1, 2)$ are two linear natural frequencies of the thin plate, $p_k^* (k = 1, 2)$ are the critical forces corresponding to two buckling modes at which thin plate loses the stability, $\omega_k^* \ (k = 1, 2)$ are the natural frequencies of the two buckling modes, and $f_k (k = 1, 2)$ are the amplitudes of parametric excitation.

3. PERTURBATION ANALYSIS

The method of multiple scales [17] may be used to find the uniform solutions of equations (10) in the following form:

$$x_n(t, \varepsilon) = x_{n0}(T_0, T_1) + \varepsilon x_{n1}(T_0, T_1) + \cdots, \quad n = 1, 2, \tag{12}$$

where $T_0 = t$, $T_1 = \varepsilon t$. Then we have the differential operators

$$\frac{\mathrm{d}}{\mathrm{d}t} = \frac{\partial}{\partial T_0}\frac{\partial T_0}{\partial t} + \frac{\partial}{\partial T_1}\frac{\partial T_1}{\partial t} + \cdots = D_0 + \varepsilon D_1 + \cdots, \tag{13}$$

$$\frac{\mathrm{d}^2}{\mathrm{d}t^2} = (D_0 + \varepsilon D_1 + \cdots)^2 = D_0^2 + 2\varepsilon D_0 D_1 + \cdots, \tag{14}$$

where $D_k = \partial/\partial T_k$, $k = 0, 1$.

We only study the case of primary parametric resonance and 1 : 1 internal resonance. In this resonant case these are the following relations:

$$\omega_1^2 = \tfrac{1}{4}\Omega^2 + \varepsilon\sigma_1 \quad \text{and} \quad \omega_2^2 = \tfrac{1}{4}\Omega^2 + \varepsilon\sigma_2, \tag{15}$$

where σ_1 and σ_2 are the two detuning parameters. For convenience of the study, we let $\Omega = 2$.

Substituting equations (12)–(14) into equations (10) and balancing the coefficients of like power of ε on the left- and right-hand side of the equations, the differential equations are obtained as follows:

order ε^0

$$D_0^2 x_{10} + x_{10} = 0, \tag{16}$$

$$D_0^2 x_{20} + x_{20} = 0. \tag{17}$$

order ε

$$\begin{aligned} D_0^2 x_{11} + x_{11} = &- 2D_0 D_1 x_{10} - \mu D_0 x_{10} - \sigma_1 x_{10} - 2f_1 x_{10}\cos 2T_0 \\ &- \alpha_1 x_{10}^3 - \alpha_2 x_{10} x_{20}^2, \end{aligned} \tag{18}$$

$$\begin{aligned} D_0^2 x_{21} + x_{21} = &- 2D_0 D_1 x_{20} - \mu D_0 x_{20} - \sigma_2 x_{20} - 2f_2 x_{20}\cos 2T_0 \\ &- \beta_1 x_{20}^3 - \beta_2 x_{10}^2 x_{20}, \end{aligned} \tag{19}$$

The solutions in the complex form of equations (16) and (17) can be found as

$$x_{n0} = A_n(T_1)e^{iT_0} + \bar{A}_n(T_1)e^{-iT_0}, \tag{20}$$

where $n = 1$, 2, and $\bar{A}$ is the complex conjugate of A. Substituting equation (20) into equations (18) and (19) yields

$$\begin{aligned} D_0^2 x_{11} + x_{11} = [&- 2iD_1A_1 - i\mu A_1 - \sigma_1 A_1 - f_1\bar{A}_1 - 3\alpha_1 A_1^2\bar{A}_1 - 2\alpha_2 A_1 A_2 \bar{A}_2 \\ &- \alpha_2 \bar{A}_1 A_2^2]e^{iT_0} + \mathrm{cc} + \mathrm{NST}, \end{aligned} \tag{21}$$

$$\begin{aligned} D_0^2 x_{21} + x_{21} = [&- 2iD_1A_2 - i\mu A_2 - \sigma_2 A_2 - f_2\bar{A}_2 - 3\beta_1 A_2^2\bar{A}_2 - 2\beta_2 A_1 \bar{A}_1 A_2 \\ &- \beta_2 A_1^2 \bar{A}_2]e^{iT_0} + \mathrm{cc} + \mathrm{NST}, \end{aligned} \tag{22}$$

where cc represents the parts of the complex conjugate of the function on the right-hand side of equations (21) and (22), and NST represents the terms that do not produce secular terms. Eliminating the terms that produce secular terms from equations (21) and (22) yields

$$D_1A_1 = -\tfrac{1}{2}\mu A_1 + \tfrac{1}{2}i\sigma_1 A_1 + \tfrac{1}{2}if_1\bar{A}_1 + \tfrac{3}{2}i\alpha_1 A_1^2\bar{A}_1 + i\alpha_2 A_1 A_2\bar{A}_2 + \tfrac{1}{2}i\alpha_2\bar{A}_1 A_2^2, \tag{23}$$

$$D_1A_2 = -\tfrac{1}{2}\mu A_2 + \tfrac{1}{2}i\sigma_2 A_2 + \tfrac{1}{2}if_2\bar{A}_2 + \tfrac{3}{2}i\beta_1 A_2^2\bar{A}_2 + i\beta_2 A_1 \bar{A}_1 A_2 + \tfrac{1}{2}i\beta_2 A_1^2\bar{A}_2. \tag{24}$$

The functions A_n ($n = 1, 2$) may be expressed in the polar form

$$A_n = \tfrac{1}{2}a_n e^{i\varphi_n} \quad \text{and} \quad n = 1, 2, \tag{25}$$

where a_n and φ_n are the real functions with respect to T_1. Substituting equation (25) into equations (23) and (24), the averaged equations in the polar form are obtained as follows:

$$\begin{aligned} \frac{da_1}{dT_1} &= -\tfrac{1}{2}\mu a_1 + \tfrac{1}{2}f_1 a_1 \sin 2\varphi_1 + \tfrac{1}{8}\alpha_2 a_1 a_2^2 \sin 2(\varphi_1 - \varphi_2), \\ a_1\frac{d\varphi_1}{dT_1} &= \tfrac{1}{2}\sigma_1 a_1 + \tfrac{3}{8}\alpha_1 a_1^3 + \tfrac{1}{4}\alpha_2 a_1 a_2^2 + \tfrac{1}{2}f_1 a_1 \cos 2\varphi_1 + \tfrac{1}{8}\alpha_2 \alpha_1 a_2^2 \cos 2(\varphi_1 - \varphi_2), \\ \frac{da_2}{dT_1} &= -\tfrac{1}{2}\mu a_2 + \tfrac{1}{2}f_2 a_2 \sin 2\varphi_2 + \tfrac{1}{8}\beta_2 a_1^2 a_2 \sin 2(\varphi_1 - \varphi_2), \\ a_2\frac{d\varphi_2}{dT_1} &= \tfrac{1}{2}\sigma_2 a_2 + \tfrac{3}{8}\beta_1 a_2^3 + \tfrac{1}{4}\beta_2 a_1^2 a_2 + \tfrac{1}{2}f_2 a_2 \cos 2\varphi_2 + \tfrac{1}{8}\beta_2 a_1^2 a_2 \cos 2(\varphi_1 - \varphi_2). \end{aligned} \tag{26}$$

It is noted from equation (26) that the periodic solutions and local bifurcation of the thin plate can be analyzed when

$$\frac{da_1}{dT_1} = \frac{d\varphi_1}{dT_1} = \frac{da_2}{dT_1} = \frac{d\varphi_2}{dT_1} = 0.$$

4. NORMAL FORM OF AVERAGED EQUATIONS

In order to obtain the normal form of averaged equations and analyze the global bifurcations, we need to transform the averaged equations from the polar form into

Cartesian form. Let

$$x_1 = \tfrac{1}{2}a_1 \cos\varphi_1, \quad x_2 = \tfrac{1}{2}a_1 \sin\varphi_1, \quad x_3 = \tfrac{1}{2}a_2 \cos\varphi_2, \quad x_4 = \tfrac{1}{2}a_2 \sin\varphi_2. \tag{27}$$

Then, equations (26) can be transformed into the following Cartesian form:

$$\begin{aligned}
\frac{dx_1}{dT_1} &= -\tfrac{1}{2}\mu x_1 - \tfrac{1}{2}(\sigma_1 - f_1)x_2 - \tfrac{3}{2}\alpha_1 x_2(x_1^2 + x_2^2) - \tfrac{1}{2}\alpha_2 x_2(x_3^2 + 3x_4^2) - \alpha_2 x_1 x_3 x_4,\\
\frac{dx_2}{dT_1} &= \tfrac{1}{2}(\sigma_1 + f_1)x_1 - \tfrac{1}{2}\mu x_2 + \tfrac{3}{2}\alpha_1 x_1(x_1^2 + x_2^2) + \tfrac{1}{2}\alpha_2 x_1(3x_3^2 + x_4^2) + \alpha_2 x_2 x_3 x_4,\\
\frac{dx_3}{dT_1} &= -\tfrac{1}{2}\mu x_3 - \tfrac{1}{2}(\sigma_2 - f_2)x_4 - \tfrac{3}{2}\beta_1 x_4(x_3^2 + x_4^2) - \tfrac{1}{2}\beta_2 x_4(x_1^2 + 3x_2^2) - \beta_2 x_1 x_2 x_3,\\
\frac{dx_4}{dT_1} &= \tfrac{1}{2}(\sigma_2 + f_2)x_3 - \tfrac{1}{2}\mu x_4 + \tfrac{3}{2}\beta_1 x_3(x_3^2 + x_4^2) + \tfrac{1}{2}\beta_2 x_3(3x_1^2 + x_2^2) + \beta_2 x_1 x_2 x_4.
\end{aligned} \tag{28}$$

We notice that the averaged equations (28) have the $Z_2 \oplus Z_2$ and D_4 symmetries. It is known that system (28) has a trivial zero solution $(x_1, x_2, x_3, x_4) = (0, 0, 0, 0)$ at which the Jacobi matrix can be written as

$$J = D_x X = \begin{bmatrix} -\tfrac{1}{2}\mu & -\tfrac{1}{2}(\sigma_1 - f_1) & 0 & 0 \\ \tfrac{1}{2}(\sigma_1 + f_2) & -\tfrac{1}{2}\mu & 0 & 0 \\ 0 & 0 & -\tfrac{1}{2}\mu & -\tfrac{1}{2}(\sigma_2 - f_2) \\ 0 & 0 & \tfrac{1}{2}(\sigma_2 + f_2) & -\tfrac{1}{2}\mu \end{bmatrix}. \tag{29}$$

The characteristic equation corresponding to the trivial zero solution is

$$(\lambda^2 + 2\mu\lambda + \sigma_1^2 + \mu^2 - f_1^2)(\lambda^2 + 2\mu\lambda + \sigma_2^2 + \mu^2 - f_2^2) = 0. \tag{30}$$

Let

$$\Delta_1 = \sigma_1^2 + \mu^2 - f_1^2 \quad \text{and} \quad \Delta_2 = \sigma_2^2 + \mu^2 - f_2^2. \tag{31}$$

When $\mu = 0$, $\Delta_1 = 0$ and $\Delta_2 = \sigma_2^2 - f_2^2 > 0$ simultaneously, system (28) has one non-semisimple double zero and a pair of pure imaginary eigenvalues

$$\lambda_{1,2} = 0 \quad \text{and} \quad \lambda_{3,4} = \pm\, \mathrm{i}\omega, \tag{32}$$

where $\omega^2 = \sigma_2^2 - f_2^2$. Considering the excitation amplitude f_2 as a parameter, and letting $\sigma_1 = -f_1 + 2\bar{\sigma}_1$ as well as setting $f_1 = 1$, then equations (28) which do not have the parameters become as follows:

$$\frac{dx_1}{dT_1} = x_2 - \tfrac{3}{2}\alpha_1 x_2(x_1^2 + x_2^2) - \tfrac{1}{2}\alpha_2 x_2(x_3^2 + 3x_4^2) - \alpha_2 x_1 x_3 x_4,$$

$$\frac{dx_2}{dT_1} = \tfrac{3}{2}\alpha_1 x_1(x_1^2 + x_2^2) + \tfrac{1}{2}\alpha_2 x_1(3x_3^2 + x_4^2) + \alpha_2 x_2 x_3 x_4,$$

$$\frac{dx_3}{dT_1} = -\tfrac{1}{2}\sigma_2 x_4 - \tfrac{3}{2}\beta_1 x_4(x_3^2 + x_4^2) - \tfrac{1}{2}\beta_2 x_4(x_1^2 + 3x_2^2) - \beta_2 x_1 x_2 x_3, \tag{33}$$

$$\frac{dx_4}{dT_1} = \tfrac{1}{2}\sigma_2 x_3 + \tfrac{3}{2}\beta_1 x_3(x_3^2 + x_4^2) + \tfrac{1}{2}\beta_2 x_3(3x_1^2 + x_2^2) + \beta_2 x_1 x_2 x_4.$$

Based on the above analysis, a near-identity non-linear transformation can be introduced as follows:

$$x_1 = y_1 - \tfrac{1}{4}\alpha_1 y_1^3 - \frac{\alpha_2}{2\sigma_2} y_1(y_3^2 - y_4^2) + \frac{\alpha_2}{2\sigma_2^2} y_1(y_3^2 - y_4^2) + \left(\frac{\alpha_2}{\sigma_2} - \frac{2\alpha_2}{\sigma_2^2} + \frac{2\alpha_2}{\sigma_2^3}\right) y_2 y_3 y_4,$$

$$x_2 = y_2 + \frac{3\alpha_1}{4} y_2(y_1^2 + 2y_2^2) + \frac{\alpha_2}{2\sigma_2} y_2(y_3^2 - y_4^2) - \frac{\alpha_2}{2\sigma_2^2} y_2(y_3^2 - y_4^2)$$

$$+ \alpha_2 y_2(y_3^2 + y_4^2) + \frac{\alpha_2}{\sigma_2} y_1 y_3 y_4, \tag{34}$$

$$x_3 = y_3 - \frac{\beta_2}{2\sigma_2} y_3(y_1^2 - y_2^2) - \left(\frac{\beta_2}{\sigma_2^2} - \frac{\beta_2}{\sigma_2^3}\right) y_2^2 y_3 - \left(\beta_2 - \frac{\beta_2}{\sigma_2} + \frac{\beta_2}{\sigma_2^2}\right) y_1 y_2 y_4,$$

$$x_4 = y_4 + \frac{\beta_2}{2\sigma_2} y_4(y_1^2 - y_2^2) - \left(\frac{\beta_2}{\sigma_2^2} - \frac{\beta_2}{\sigma_2^3}\right) y_2^2 y_4 + \left(\beta_2 + \frac{\beta_2}{\sigma_2} - \frac{\beta_2}{\sigma_2^2}\right) y_1 y_2 y_3.$$

Then, with the aid of Maple program [18], the normal form of equations (33) can be obtained as follows:

$$\dot{y}_1 = y_2, \quad \dot{y}_2 = \tfrac{3}{2}\alpha_1 y_1^3 + \alpha_2 y_1(y_3^2 + y_4^2),$$

$$\dot{y}_3 = -\tfrac{1}{2}\sigma_2 y_4 - \tfrac{3}{2}\beta_1 y_4(y_3^2 + y_4^2) - \beta_2 y_1^2 y_4, \tag{35}$$

$$\dot{y}_4 = \tfrac{1}{2}\sigma_2 y_3 + \tfrac{3}{2}\beta_1 y_3(y_3^2 + y_4^2) + \beta_2 y_1^2 y_3,$$

where a dot denotes the derivative with respect to T_1. The normal form with parameters can be written as

$$\dot{y}_1 = -\bar{\mu} y_1 + (1 - \bar{\sigma}_1) y_2,$$

$$\dot{y}_2 = \bar{\sigma}_1 y_1 - \bar{\mu} y_2 + \tfrac{3}{2}\alpha_1 y_1^3 + \alpha_2 y_1(y_3^2 + y_4^2),$$

$$\dot{y}_3 = -\bar{\mu} y_3 - (\bar{\sigma}_2 - f_2) y_4 - \tfrac{3}{2}\beta_1 y_4(y_3^2 + y_4^2) - \beta_2 y_1^2 y_4, \tag{36}$$

$$\dot{y}_4 = (\bar{\sigma}_2 + f_2) y_3 - \bar{\mu} y_4 + \tfrac{3}{2}\beta_1 y_3(y_3^2 + y_4^2) + \beta_2 y_1^2 y_3,$$

where $\bar{\sigma}_2 = \frac{1}{2}\sigma_2, \bar{f}_2 = \frac{1}{2}f_2$ and $\bar{\mu} = \frac{1}{2}\mu$. Further, letting

$$y_3 = I\cos\gamma \quad \text{and} \quad y_4 = I\sin\gamma, \tag{37}$$

and substituting equation (37) into normal form (36) can yield

$$\begin{aligned}
\dot{y}_1 &= -\bar{\mu}y_1 + (1-\bar{\sigma}_1)y_2, \\
\dot{y}_2 &= \bar{\sigma}_1 y_1 - \bar{\mu}y_2 + \tfrac{3}{2}\alpha_1 y_1^3 + \alpha_2 y_1 I^2, \\
\dot{I} &= -\bar{\mu}I + \bar{f}_2 I\sin 2\gamma, \\
I\dot{\gamma} &= \bar{\sigma}_2 I + \tfrac{3}{2}\beta_1 I^3 + \beta_2 I y_1^2 + \bar{f}_2 I\cos 2\gamma.
\end{aligned} \tag{38}$$

Introducing a linear transformation

$$\begin{bmatrix} y_1 \\ y_2 \end{bmatrix} = \begin{bmatrix} 1-\bar{\sigma}_1 & 0 \\ \bar{\mu} & 1 \end{bmatrix}\begin{bmatrix} u_1 \\ u_2 \end{bmatrix}, \tag{39}$$

yields

$$\begin{bmatrix} u_1 \\ u_2 \end{bmatrix} = \frac{1}{1-\bar{\sigma}_1}\begin{bmatrix} 1 & 0 \\ -\bar{\mu} & 1-\bar{\sigma}_1 \end{bmatrix}\begin{bmatrix} y_1 \\ y_2 \end{bmatrix}. \tag{40}$$

Substituting equations (39) and (40) into equations (38) and omitting the non-linear terms with the parameter $\bar{\sigma}_1$ yields the unfolding as

$$\begin{aligned}
\dot{u}_1 &= u_2, \\
\dot{u}_2 &= -\mu_1 u_1 - \mu_2 u_2 + \alpha_2 I^2 u_1 + \tfrac{3}{2}\alpha_1 u_1^3, \\
\dot{I} &= -\bar{\mu}I + \bar{f}_2 I\sin 2\gamma, \\
I\dot{\gamma} &= \bar{\sigma}_2 I + \tfrac{3}{2}\beta_1 I^3 + \beta_2 I u_1^2 + \bar{f}_2 I\cos 2\gamma,
\end{aligned} \tag{41}$$

where $\mu_1 = \bar{\mu}^2 - \bar{\sigma}_1(1-\bar{\sigma}_1)$ and $\mu_2 = 2\bar{\mu}$.

The scale transformations may be introduced as follows:

$$\mu_2 \to \varepsilon\mu_2, \quad \bar{\mu} \to \varepsilon\bar{\mu}, \quad \bar{f}_2 \to \varepsilon\bar{f}_2, \quad \tfrac{3}{2}\alpha_1 \to \alpha_1, \quad \tfrac{3}{2}\beta_1 \to \beta_1. \tag{42}$$

Then, normal form (41) can be rewritten as the form with the perturbation

$$\begin{aligned}
\dot{u}_1 &= \frac{\partial H}{\partial u_2} + \varepsilon g^{u_1} = u_2, \\
\dot{u}_2 &= -\frac{\partial H}{\partial u_1} + \varepsilon g^{u_2} = -\mu_1 u_1 + \alpha_1 u_1^3 + \alpha_2 u_1 I^2 - \varepsilon\mu_2 u_2, \\
\dot{I} &= \frac{\partial H}{\partial \gamma} + \varepsilon g^{I} = -\varepsilon\bar{\mu}I + \varepsilon\bar{f}_2 I\sin 2\gamma, \\
I\dot{\gamma} &= -\frac{\partial H}{\partial I} + \varepsilon g^{\gamma} = \bar{\sigma}_2 I + \beta_1 I^3 + \beta_2 u_1^2 I + \varepsilon\bar{f}_2 I\cos 2\gamma,
\end{aligned} \tag{43}$$

where the Hamiltonian function is of the form

$$H(u_1, u_2, I, \gamma) = \tfrac{1}{2}u_2^2 + \tfrac{1}{2}\mu_1 u_1^2 - \tfrac{1}{4}\alpha_1 u_1^4 - \tfrac{1}{2}\alpha_2 I^2 u_1^2 - \tfrac{1}{2}\bar{\sigma}_2 I^2 - \tfrac{1}{4}\beta_1 I^4, \tag{44}$$

and $\alpha_2 = \beta_2$, $g^{u_1} = 0$, $g^{u_2} = -\mu_2 u_2$, $g^I = -\mu I + \bar{f}_2 I \sin 2\gamma$ and $g^\gamma = \bar{f}_2 I \cos 2\gamma$.

It is noted that unfolding, equation (43) with the perturbation is similar to the equations studied by Wiggins [19] as well as Kovicic and Wiggins [4]. But there are differences between this paper and the papers [4, 19]. It is observed from the papers [4, 19] that the researchers investigated the case in which the first two equations have a pair of pure imaginary eigenvalues. In this paper, first, the autonomous system can be further simplified by the normal form. Then, it is considered that system (28) has one non-semisimple double zero and a pair of pure imaginary eigenvalues. In references [3, 20] the researchers used a series of non-linear transformations to obtain the standard form of equations. It is observed that the normal form with perturbation is actually simpler than the standard form of equations when we analyze the singular points, the stability of system, and calculate Melnikov function. So it is easier and more convenient for one to use the theory of normal form to simplify the equations to the standard form of equations and to analyze the dynamics of the simplified equations.

5. ANALYSIS OF GLOBAL BIFURCATIONS

5.1. DYNAMICS OF DECOUPLED SYSTEM

When $\varepsilon = 0$, it is noted that system (43) is a two uncoupled single-d.o.f. non-linear system. The I variable appears in (u_1, u_2) components of system (43) as a parameter since $\dot{I} = 0$. Consider the first two decoupled equations with perturbation term

$$\dot{u}_1 = u_2, \quad \dot{u}_2 = -\mu_1 u_1 + \alpha_2 I^2 u_1 + \alpha_1 u_1^3 - \varepsilon\mu_2 u_2. \tag{45}$$

Since $\alpha_1 > 0$, system (45) can exhibit the heteroclinic bifurcations. It is easy to see from equations (45) that when $\mu_1 - \alpha_2 I^2 < 0$, the only solution of system (45) is the trivial zero solution $(u_1, u_2) = (0, 0)$ which is the saddle point. On the curve defined by $\mu_1 = \alpha_2 I^2$, that is,

$$\bar{\mu}^2 = \bar{\sigma}_1(1 - \bar{\sigma}_1) + \alpha_2 I^2 \tag{46}$$

or

$$I_{1,2} = \pm\left[\frac{\bar{\mu}^2 - \bar{\sigma}_1(1 - \bar{\sigma}_1)}{\alpha_2}\right]^{1/2}, \tag{47}$$

the trivial zero solution may bifurcate into three solutions through a pitchfork bifurcation, which are given by $q_0 = (0, 0)$ and $q_\pm(I) = (B, 0)$, respectively, where

$$B = \pm\left\{\frac{1}{\alpha_1}[\bar{\mu}^2 - \bar{\sigma}_1(1 - \bar{\sigma}_1) - \alpha_2 I^2]\right\}^{1/2}. \tag{48}$$

From the Jacobian matrix evaluated at the non-zero solutions, it is known that the singular points $q_\pm(I)$ are the saddle points. On the line $\mu_2 = 0$, the Hopf bifurcation can occur from the trivial zero solution. The simple analysis for Hopf bifurcation shows that when $\mu_2 < 0$, the limit cycle is stable.

It is observed that I and γ may represent actually the amplitude and phase of the vibrations. Therefore, we may assume that $I \geqslant 0$ and equation (47) becomes

$$I_1 = 0 \quad \text{and} \quad I_2 = \left[\frac{\bar{\mu}^2 - \bar{\sigma}_1(1-\bar{\sigma}_1)}{\alpha_2}\right]^{1/2}, \tag{49}$$

such that for all $I \in [I_1, I_2]$, system (45) has two hyperbolic saddle points, $q_\pm(I)$, which are connected by a pair of heteroclinic orbits, $u^h_\pm(T_1, I)$, that is, $\lim_{T_1 \to \pm\infty} u^h_\pm(T_1, I) = q_\pm(I)$. So in the full four-dimensional phase space the set defined by

$$M = \{(u, I, \gamma) | u = q_\pm(I), \quad I_1 \leqslant I \leqslant I_2, \quad 0 \leqslant \gamma \leqslant 2\pi\} \tag{50}$$

is a two-dimensional invariant manifold. From the results obtained in references [4, 19, 20], it is known that the two-dimensional invariant manifold M is normally hyperbolic. The two-dimensional normally hyperbolic invariant manifold M has three-dimensional stable and unstable manifolds which are represented as $W^s(M)$ and $W^u(M)$ respectively. The existence of the heteroclinic orbit of system (45) to $q_\pm(I) = (B, 0)$ indicates that $W^s(M)$ and $W^u(M)$ intersect non-transversally along a three-dimensional heteroclinic manifold denoted by Γ [4], which can be written as

$$\Gamma = \left\{(u, I, \gamma) | u = u^h_\pm(T_1, I),\, I_1 < I < I_2,\, \gamma = \int_0^{T_1} D_I H(u^h_\pm(T_1, I), I)\,\mathrm{d}s + \gamma_0\right\}. \tag{51}$$

Now we analyze the dynamics of the unperturbed system of equations (43) restricted to M. Considering the unperturbed system of equations (43) restricted to M yields

$$\dot{I} = 0, \quad I\dot{\gamma} = D_I H(q_\pm(I), I), \quad I_1 \leqslant I \leqslant I_2, \tag{52}$$

where

$$D_I H(q_\pm(I), I) = -\frac{\partial H(q_\pm(I), I)}{\partial I} = \bar{\sigma}_2 I + \beta_1 I^3 + \beta_2 I q^2_\pm(I).$$

From Kovacic and Wiggins [4], it is known that if $D_I H(q_\pm(I), I) \neq 0$ then $I =$ constant is called as a periodic orbit and if $D_I H(q_\pm(I), I) = 0$ then $I =$ constant is called as a circle of the singular points. A value of $I \in [I_1, I_2]$ at which $D_I H(q_\pm(I), I) = 0$ is called as a resonant I value and these singular points as resonant singular points. We denote a resonant value by I_r so that

$$D_I H(q_\pm(I), I) = \bar{\sigma}_2 I_r + \beta_1 I_r^3 + \frac{\beta_2 I_r}{\alpha_1}[\bar{\mu}^2 - \bar{\sigma}_1(1-\bar{\sigma}_1) - \alpha_2 I_r^2] = 0. \tag{53}$$

Then, we obtain

$$I_r = \pm\left\{\frac{\alpha_1\bar{\sigma}_2 + \beta_2[\bar{\mu}^2 - \bar{\sigma}_1(1-\bar{\sigma}_1)]}{\alpha_2\beta_2 - \alpha_1\beta_1}\right\}^{1/2}. \tag{54}$$

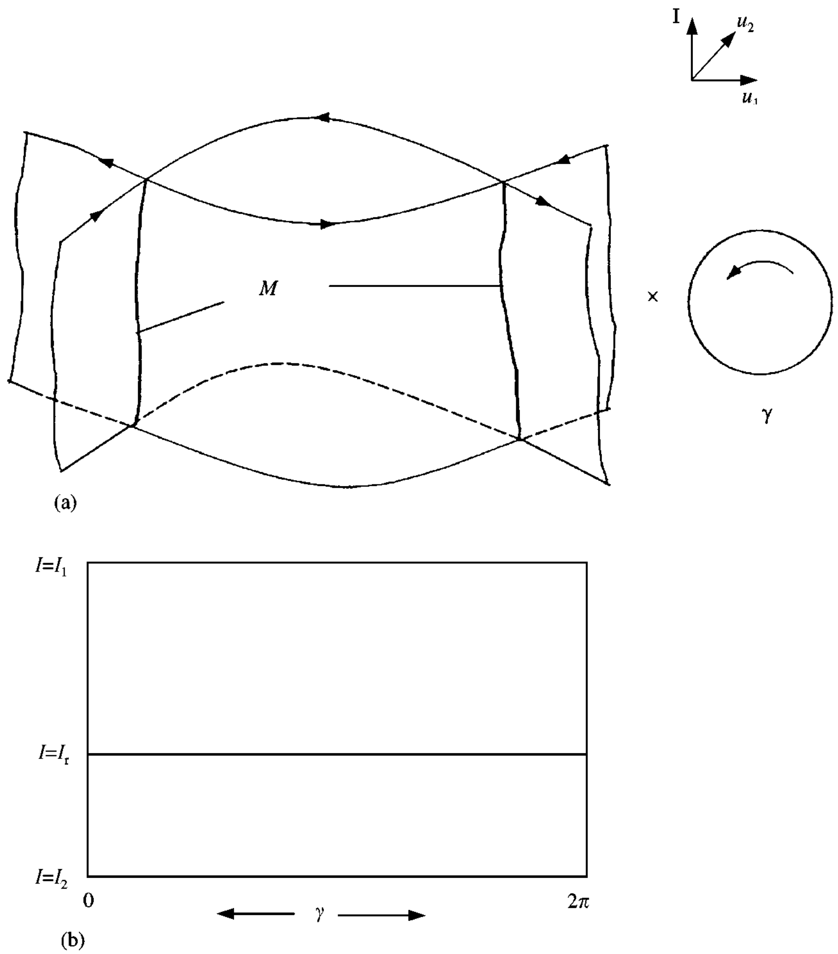

Figure 2. The geometric structure of M, $W^s(M)$ and $W^u(M)$ in the full four-dimensional phase space.

The geometry structure of the stable and unstable manifolds of M in the full four-dimensional phase space for the unperturbed system of equations (43) is given in Figure 2. Because γ may represent the phase of the oscillations, when $I = I_r$, the phase shift $\Delta\gamma$ of the oscillations is defined as

$$\Delta\gamma = \gamma(+\infty, I_r) - \gamma(-\infty, I_r). \tag{55}$$

The physical interpretation of the phase shift is the phase difference between the two end points of the orbit. In (u_1, u_2) subspace, there exist a pair of the heteroclinic orbits connecting to the two saddles. Therefore, in fact the homoclinic orbit in (I, γ) subspace is of a heteroclinic connecting in full four-dimensional phase space (u_1, u_2, I, γ). The phase shift may denote the difference of γ value as a trajectory leaves and returns to the basin of attraction of M. We will use the phase shift in subsequent analysis to obtain the condition for the existence of Silnikov-type homoclinic orbit. The phase shift will be calculated in the later analysis given for the heteroclinic orbit.

We consider the heteroclinic bifurcations of system (45). Letting $\varepsilon_1 = \mu_1 - \alpha_2 I^2$ and $\mu_2 = \varepsilon_2$, system (45) can be rewritten as

$$\dot{u}_1 = u_2, \quad \dot{u}_2 = -\varepsilon_1 u_1 + \alpha_1 u_1^3 - \varepsilon\varepsilon_2 u_2. \tag{56}$$

Setting $\varepsilon = 0$ in equations (56) we see that system (56) is a Hamiltonian system with Hamiltonian

$$H(u_1, u_2) = \tfrac{1}{2}u_2^2 + \tfrac{1}{2}\varepsilon_1 u_1^2 - \tfrac{1}{4}\alpha_1 u_1^4. \tag{57}$$

When $H = \varepsilon_1^2/4\alpha_1$, there exists a heteroclinic loop Γ^0 which consists of the two hyperbolic saddles $q_\pm$ and a pair of heteroclinic orbits $u_\pm(T_1)$. The equations of pair of heteroclinic orbits can be obtained as

$$\begin{aligned} u_1(T_1) &= \pm\sqrt{\varepsilon_1 \alpha_1}\tanh\left(\frac{\sqrt{2\varepsilon_1}}{2}T_1\right) \\ u_2(T_1) &= \pm\frac{\varepsilon_1}{\sqrt{2\alpha_1}}\operatorname{sech}^2\left(\frac{\sqrt{2\varepsilon_1}}{2}T_1\right). \end{aligned} \tag{58}$$

The Melnikov function for heteroclinic orbits is easily given by

$$M(\varepsilon_1, \varepsilon_2, I) = \int_{-\infty}^{\infty} u_2(T_1)[-\varepsilon_2 u_2(T_1)]\,\mathrm{d}T_1 = -\frac{2\sqrt{2}\varepsilon_1^{3/2}\varepsilon_2}{3\alpha_1}. \tag{59}$$

To keep the heteroclinic loop preserved under a perturbation, it is necessary to require that $M(\varepsilon_1, \varepsilon_2, I) = 0$. Therefore, equation (59) leads to $\varepsilon_2 = 0$ which corresponds to the singular point, or $\varepsilon_1 = 0$. Choosing $\varepsilon_1 = 0$, then, a heteroclinic bifurcation curve can be obtained as

$$\bar{\mu}^2 = \bar{\sigma}_1(1 - \bar{\sigma}_1) + \alpha_2 I^2. \tag{60}$$

It is found from equations (46) and (60) that the pitchfork bifurcation curve and the heteroclinic bifurcation curve coincide. Based on equations (46) and (60), the bifurcation diagram of system (45) is obtained in Figure 3, and the corresponding phase portraits are given in Figure 4.

Let us turn our attention to the computation of the phase shift. Substituting the first equation of equations (58) into the fourth equation of the unperturbed system of equations (43) yields

$$\dot{\gamma} = \bar{\sigma}_2 + \beta_1 I^2 + \frac{\varepsilon_1\beta_2}{\alpha_1}\tanh^2\left(\frac{\sqrt{2\varepsilon_1}}{2}T_1\right). \tag{61}$$

Integrating equation (61) yields

$$\gamma(T_1) = \omega_r T_1 - \frac{\beta_2\sqrt{2\varepsilon_1}}{\alpha_1}\tanh\left(\frac{\sqrt{2\varepsilon_1}}{2}T_1\right) + \gamma_0, \tag{62}$$

where $\omega_r = \bar{\sigma}_2 + \beta_1 I^2 + \varepsilon_1\beta_2/\alpha_1$.

At $I = I_r$, there is $\omega_r \equiv 0$. Therefore, the phase shift may be expressed as

$$\Delta\gamma = \left[-\frac{2\beta_2\sqrt{2\varepsilon_1}}{\alpha_1}\right]_{I=I_r} = -\frac{2\beta_2}{\alpha_1}\sqrt{2[\bar{\mu}^2 - \bar{\sigma}_1(1-\bar{\sigma}_1) - \alpha_2 I_r^2]}. \tag{63}$$

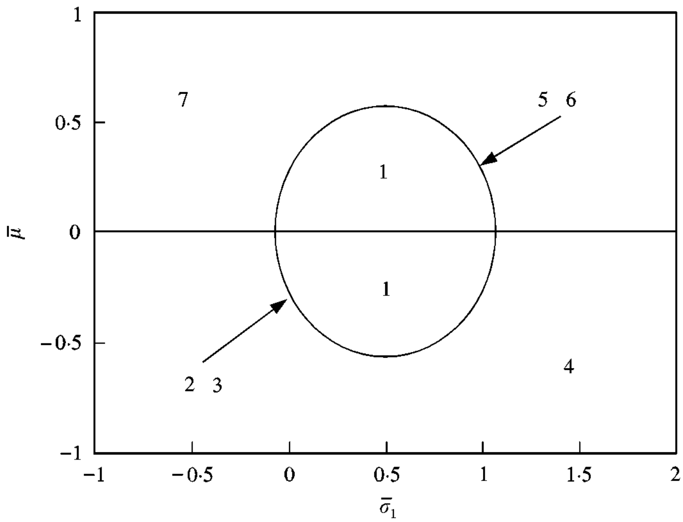

Figure 3. The bifurcation set of system (45): (1) saddle point, (2) stable limit cycle, (3) heteroclinic loop, (4) heteroclinic orbit, (5) unstable limit cycle, (6) heteroclinic loop, and (7) heteroclinic orbit.

5.2. GLOBAL ANALYSIS OF PERTURBED SYSTEM

In this section, we analyze the dynamics of the perturbed system and the effect of small perturbations on M. Based on the analysis in references [4, 19, 20], we know that M along with its stable and unstable manifolds are invariant under small, sufficiently differentiable perturbations. It is noticed $q_\pm(I)$ may persist under small perturbations, in particular, $M \to M_\varepsilon$. So we obtain

$$M = M_\varepsilon = \{(u, I, \gamma) | u = q_\pm(I), \quad I_1 \leqslant I \leqslant I_2, \quad 0 \leqslant \gamma < 2\pi\}. \tag{64}$$

Considering the two second equations of equations (41) yields

$$\dot{I} = -\bar{\mu} I + \bar{f}_2 I \sin 2\gamma, \quad \dot{\gamma} = \bar{\sigma}_2 + \tfrac{3}{2}\beta_1 I^2 + \beta_2 u_1^2 + \bar{f}_2 \cos 2\gamma. \tag{65}$$

In this paper, it is known from the above analysis that the last two equations of equations (41) are of a pair of pure imaginary eigenvalues. So the resonance can occur in system (65). Also introduce the scale transformations

$$\bar{\mu} \to \varepsilon\bar{\mu}, \quad \beta_1 \to \tfrac{3}{2}\beta_1, \quad I = I_r + \sqrt{\varepsilon} h, \quad \bar{f}_2 \to \varepsilon f_2, \quad T_1 \to \frac{T_1}{\sqrt{\varepsilon}}. \tag{66}$$

Substituting the above transformations into equations (65) yields

$$\dot{h} = -\bar{\mu} I_r + \bar{f}_2 I_r \sin 2\gamma + \sqrt{\varepsilon}(\bar{f}_2 h \sin 2\gamma - \bar{\mu} h),$$

$$\dot{\gamma} = -\frac{2\delta}{\alpha_1} I_r h + \sqrt{\varepsilon}\left(\bar{f}_2 \cos 2\gamma - \frac{\delta}{\alpha_1} h^2\right), \tag{67}$$

with $\delta = \alpha_2\beta_2 - \alpha_1\beta_1$. When $\varepsilon = 0$, equations (67) may become

$$\dot{h} = -\bar{\mu} I_r + \bar{f}_2 I_r \sin 2\gamma, \quad \dot{\gamma} = -\frac{2\delta}{\alpha_1} I_r h. \tag{68}$$

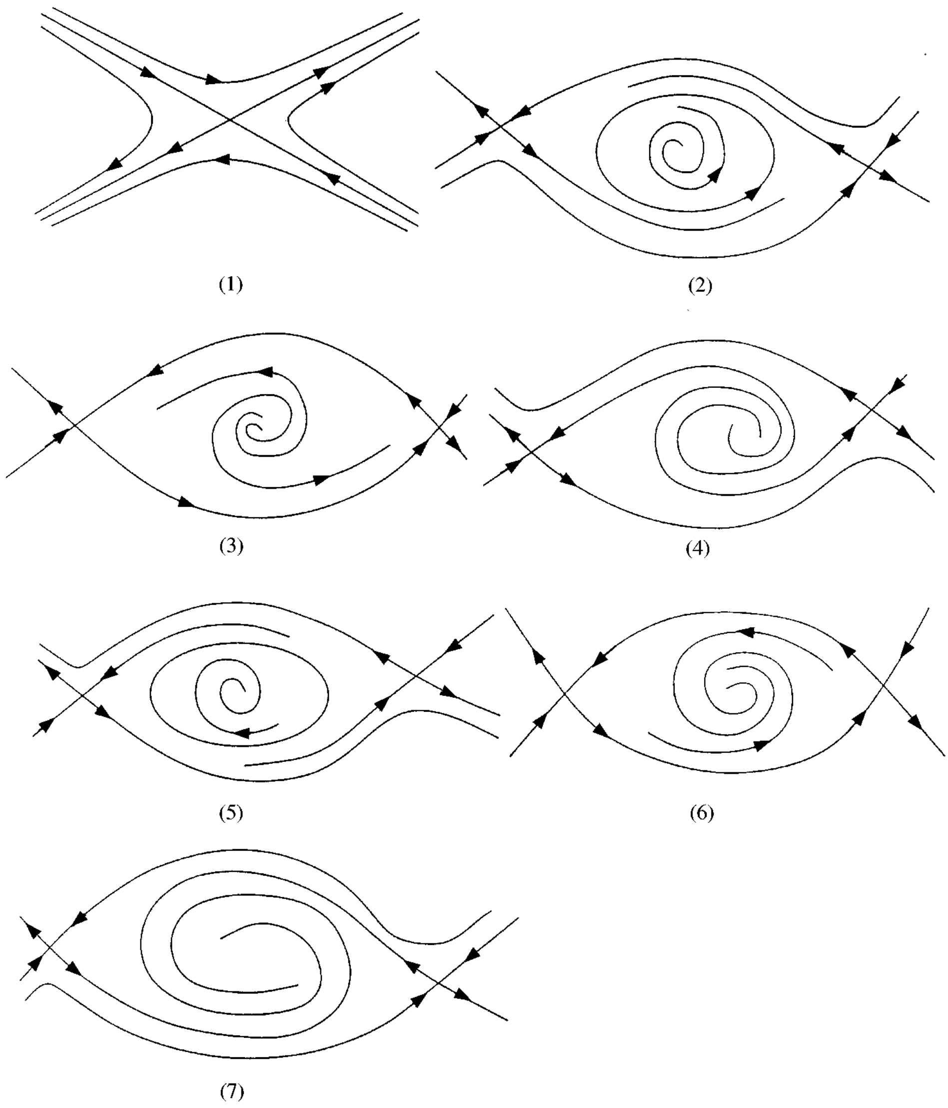

Figure 4. The phase portraits in the different bifurcation regions.

The unperturbed system (68) is a Hamiltonian system with Hamiltonian function

$$H(h, \gamma) = -\bar{\mu} I_r \gamma - \tfrac{1}{2}\bar{f}_2 I_r \cos 2\gamma + \frac{\delta}{\alpha_1} I_r h^2. \tag{69}$$

The singular points of system (68) are

$$p_0 = (0, \gamma_c) = \left(0, \tfrac{1}{2}\arcsin\frac{\bar{\mu}}{\bar{f}_2}\right) \quad \text{and} \quad q_0 = (0, \gamma_2) = \left(0, \tfrac{1}{2}\pi + \tfrac{1}{2}\arcsin\frac{\bar{\mu}}{\bar{f}_2}\right). \tag{70}$$

Based on the Jacobian matrix evaluated at the two singular points, it is known that the singular point p_0 is a center and q_0 is a saddle which is connected to itself by a homoclinic

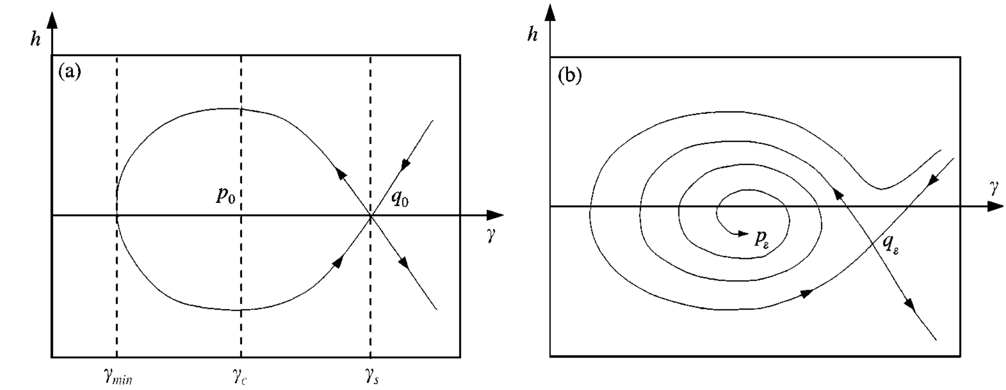

Figure 5. Dynamics on the normally hyperbolic manifold; (a) the unperturbed case, and (b) the perturbed case.

orbit. The phase portrait of system (68) is given in Figure 5(a). Following the analysis of Kovacic and Wiggins [4], it is known that for ε sufficiently small, q_0 remains a hyperbolic singular point, q_ε of saddle stability type. From equations (67), we can find that the leading order term of the trace of the linearization of equations (67) is less than zero inside the homoclinic loop. So for the small perturbations, p_0 becomes a hyperbolic sink p_ε. Also the phase portrait of the perturbed system (67) is depicted in Figure 5(b).

At $h = 0$, the estimate of basin of attraction for γ_{min} is obtained as

$$\bar{\mu}\gamma_{min} + \tfrac{1}{2}\bar{f}_2 \cos 2\gamma_{min} = \bar{\mu}\gamma_s + \tfrac{1}{2}\bar{f}_2 \cos 2\gamma_s. \tag{71}$$

Substituting γ_s of equation (70) into equation (71) yields

$$\gamma_{min} + \frac{\bar{f}_2}{2\bar{\mu}} \cos 2\gamma_{min} = \tfrac{1}{2}\pi + \tfrac{1}{2}\arcsin\frac{\bar{\mu}}{\bar{f}_2} - \frac{\sqrt{\bar{f}_2^2 - \bar{\mu}^2}}{2\bar{\mu}}. \tag{72}$$

Define an annulus A_ε near $I = I_r$ as

$$A_\varepsilon = \{(u_1, u_2, I, \gamma) | u_1 = B, u_2 = 0, |I - I_r| < \sqrt{\varepsilon}c, \gamma \in T^1\}, \tag{73}$$

where c is a constant, which is chosen sufficiently large so that the unperturbed homoclinic orbit is enclosed within the annulus. We notice that the three-dimensional stable and unstable manifolds of A_ε, denoted as $W^s(A_\varepsilon)$ and $W^u(A_\varepsilon)$, are the subset of $W^s(M_\varepsilon)$ and $W^u(M_\varepsilon)$ respectively. We will show that for the perturbed system, the saddle focus p_ε on A_ε has homoclinic orbit which comes out of the annulus A_ε and can return to the annulus in full four-dimensional space, and eventually may give rise to Silnikov-type homoclinic loop, as shown in Figure 6.

5.3. HIGHER-DIMENSIONAL MELNIKOV THEORY

In order to show the existence of Silnikov-type homoclinic orbit, we need two steps to determine it [4]. In the first step, by using higher-dimensional Melnikov theory, the measure of the distance between one-dimensional unstable manifold $W^u(p_\varepsilon)$ and three-dimensional stable manifold $W^s(A_\varepsilon)$ may be obtained to show that $W^u(p_\varepsilon) \subset W^s(A_\varepsilon)$ when Melnikov function has a simple zero. In the second step we will determine whether or

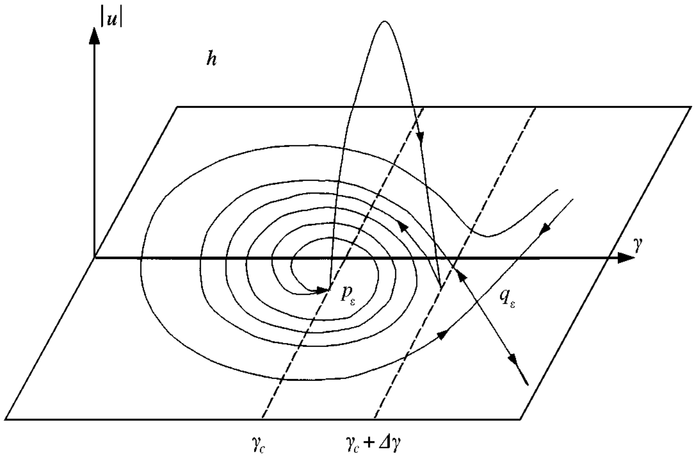

Figure 6. Silnikov-type homoclinic orbit to saddle focus.

not the orbit on $W^u(p_\varepsilon)$ comes back into the basin of attraction of A_ε. If it does, the orbit asymptotes to A_ε as $t \to \infty$. If it does not, the orbit may escape from the annulus A_ε by crossing the boundary of the annulus.

Based on the results obtained in references [4, 20], higher-dimensional Melnikov function is given as follows:

$$M(\mu_1, \bar{\sigma}_2, I_r, \bar{f}_2) = \int_{-\infty}^{+\infty} \left[\frac{\partial H}{\partial u_2} g^{u_2} + \frac{\partial H}{\partial I} g^I \right] \mathrm{d}T_1$$

$$= \int_{-\infty}^{+\infty} [-\mu_2 u_2^2(T_1) + (\bar{\sigma}_2 I_r + \beta_1 I_r^3 + \beta_2 I_r u_1^2(T_1))\,(-\bar{\mu} I_r + \bar{f}_2 I_r \sin 2\gamma(\mathrm{T}_1))]\,\mathrm{d}T_1, \quad (74)$$

where $u_1(T_1)$, $u_2(T_1)$ and $\gamma(T_1)$ are given in equations (58) and (62) respectively. From the above analysis, the first and second integrands are evaluated as follows:

$$\int_{-\infty}^{+\infty} -\mu_2 u_2^2(T_1)\,\mathrm{d}T_1 = -\frac{2\sqrt{2}\varepsilon_1^{3/2}\mu_2}{3\alpha_1}, \quad (75)$$

and

$$\int_{-\infty}^{+\infty} [-\bar{\mu} I_r(\bar{\sigma}_2 I_r + \beta_1 I_r^3 + \beta_2 I_r u_1^2(T_1))\,\mathrm{d}T_1 = -\bar{\mu} I_r^2 \Delta\gamma. \quad (76)$$

The third integral can be rewritten as

$$M_1(\mu_1, \bar{\sigma}_2, I_r, \bar{f}_2) = \bar{f}_2 I_r^2 \int_{-\infty}^{+\infty} \sin 2\gamma(T_1)(\bar{\sigma}_2 + \beta_1 I_r^2 + \beta_2 u_1^2(T_1))\,\mathrm{d}T_1$$

$$= \frac{\varepsilon_1 \beta_2 I_r^2 \bar{f}_2}{2\alpha_1} \int_{-\infty}^{+\infty} \sin 2\gamma(T_1)\,\mathrm{d}(2\gamma(T_1))$$

$$= -\frac{\varepsilon_1 \beta_2 I_r^2 \bar{f}_2}{2\alpha_1} [\cos 2\gamma(+\infty) - \cos 2\gamma(-\infty)]. \quad (77)$$

Using $\Delta\gamma = \gamma(+\infty) - \gamma(-\infty)$ yields

$$M_1(\mu_1, \bar{\sigma}_2, I_r, \bar{f}_2) = \frac{\varepsilon_1 \beta_2 I_r^2 \bar{f}_2}{2\alpha_1}[\sin 2\gamma(-\infty) \sin 2\Delta\gamma - \cos 2\gamma(-\infty)(\cos 2\Delta\gamma - 1)]. \quad (78)$$

Based on equation (70) we obtain

$$\sin 2\gamma(-\infty) = \frac{\bar{\mu}}{\bar{f}_2}, \quad \cos 2\gamma(-\infty) = \frac{\sqrt{\bar{f}_2^2 - \bar{\mu}^2}}{\bar{f}_2}. \quad (79)$$

Substituting equation (79) into equation (78), we obtain

$$M_1(\mu_1, \bar{\sigma}_2, I_r, \bar{f}_2) = \frac{\varepsilon_1 \beta_2 I_r^2}{2\alpha_1}[\bar{\mu} \sin 2\Delta\gamma - \sqrt{\bar{f}_2^2 - \bar{\mu}^2}(\cos 2\Delta\gamma - 1)]. \quad (80)$$

Therefore, the Melnikov function may be expressed as

$$M(\mu_1, \bar{\sigma}_2, I_r, \bar{f}_2) = -\frac{\sqrt{2}[\bar{\mu}^2 - \bar{\sigma}_1(1-\bar{\sigma}_1) - \alpha_2 I_r^2]^{3/2} \bar{\mu}}{3\alpha_1} - \bar{\mu} I_r^2 \Delta\gamma$$
$$+ \frac{\varepsilon_1 \beta_2 I_r^2}{2\alpha_1}[\bar{\mu} \sin 2\Delta\gamma - \sqrt{\bar{f}_2^2 - \bar{\mu}^2}(\cos 2\Delta\gamma - 1)]. \quad (81)$$

In order to determine the existence of the Silnikov-type homoclinic orbit, we first require that the Melnikov function have a simple zero. Thus, we obtain the following expression:

$$-\frac{\sqrt{2}[\bar{\mu}^2 - \bar{\sigma}_1(1-\bar{\sigma}_1) - \alpha_2 I_r^2]^{3/2} \bar{\mu}}{3\alpha_1} - \bar{\mu} I_r^2 \Delta\gamma$$
$$+ \frac{\varepsilon_1 \beta_2 I_r^2}{2\alpha_1}[\bar{\mu} \sin 2\Delta\gamma - \sqrt{\bar{f}_2^2 - \bar{\mu}^2}(\cos 2\Delta\gamma - 1)] = 0. \quad (82)$$

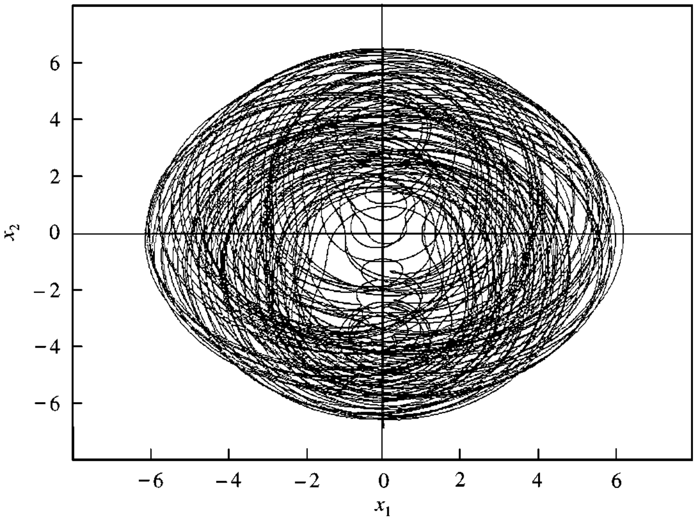

Figure 7. The chaotic response of the averaged equations (28) for $\lambda = 0{\cdot}7$ and $\mu = 0{\cdot}16$, the phase portrait on plane (x_1, x_2).

Next, we determine whether the orbit on $W^u(p_\varepsilon)$ returns to the basin of attraction of A_ε. The condition is given as

$$\gamma_{min} < \gamma_c + \Delta\gamma + m\pi < \gamma_s, \tag{83}$$

where m is an integer, $\Delta\gamma$, γ_c, γ_s and γ_{min} are given by equations (63), (70) and (72) respectively. It indicates that $W^u(p_\varepsilon) \subset W^s(A_\varepsilon)$, that is, one-dimensional unstable manifold $W^u(p_\varepsilon)$ is a subset of three-dimensional stable manifold $W^s(A_\varepsilon)$. When conditions (82) and (83) are simultaneously satisfied, it is shown that there exists the Silnikov-type chaos in system (43), that is, system (43) may give rise to chaotic dynamics in the sense of Smale horseshoes.

6. NUMERICAL SIMULATION OF CHAOS

Due to the global perturbation method developed by Kovacic and Wiggins [4] can be only used to analyze the autonomous systems but cannot be used to analyze the non-autonomous systems, thus, the original equations (10) must be transformed to autonomous averaged equations (28). From the averaged equations (28), the normal form theory is used to simplify this system to the standard form, that is, the normal form. Then, the global perturbation method is used to investigate the global bifurcations and chaotic dynamics of the normal form. For the comparison with the analytical prediction, we choose the averaged equations (28) and the original system (10) to do the numerical simulations. In addition, it is very difficult to construct the phase portraits or the topological structures of higher-dimensional non-autonomous systems.

In this section, we use the numerical method to predict the chaotic motion of the parametrically excited rectangular thin plate. A computer software called *Dynamics* [21] which can perform the analysis for ordinary differential equations is used. Consider the averaged equations (28). Firstly, the case for $\lambda = b/a = 0{\cdot}7$ is numerically studied. The other parameters are given as $\alpha_1 = 10{\cdot}3941$, $\beta_1 = 2{\cdot}6082$, and $\alpha_2 = \beta_2 = 5{\cdot}9367$. The chaotic response of the averaged equations (28) with $\mu = 0{\cdot}16$, $f_1 = 488$, $f_2 = 1169{\cdot}63$, $\sigma_1 = 3{\cdot}25$

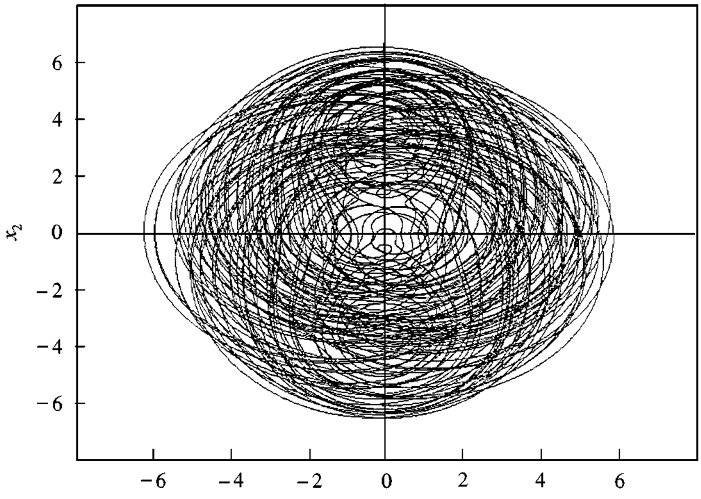

Figure 8. The chaotic response of the averaged equations (28) for $\lambda = 0{\cdot}7$ and $\mu = 0{\cdot}108$, the phase portrait on plane (x_1, x_2).

and $\sigma_2 = 6{\cdot}55$ is shown in Figure 7, which represents the phase portrait on plane (x_1, x_2). The chosen initial conditions are $x_{10} = -3{\cdot}1$, $x_{20} = 0{\cdot}8$, $x_{30} = 1{\cdot}011$ and $x_{40} = 1{\cdot}4$. The chaotic response for $\mu = 0{\cdot}108$ and $f_2 = 1239{\cdot}63$ is shown in Figure 8. Then, the case for $\lambda = 0{\cdot}9$ is also investigated and the chaotic responses of the averaged equations (28) are given in Figures 9 and 10, where the damped coefficients are $\mu = 0{\cdot}18$ and $0{\cdot}138$ respectively. The chosen parameters and initial conditions are: $\alpha_1 = 6{\cdot}3125$, $\beta_1 = 4{\cdot}1778$, $\alpha_2 = \beta_2 = 7{\cdot}3308$, $\sigma_1 = 3{\cdot}25$, $\sigma_2 = 6{\cdot}55$, $f_1 = 488$, $f_2 = 1189{\cdot}63$, $x_{10} = -3{\cdot}1$, $x_{20} = 0{\cdot}8$, $x_{30} = 1{\cdot}011$ and $x_{40} = 1{\cdot}4$.

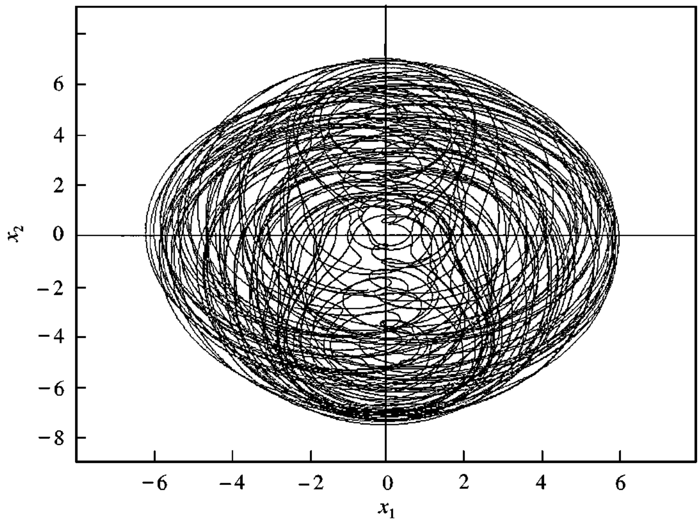

Figure 9. The chaotic response of the averaged equations (28) for $\lambda = 0{\cdot}9$ and $\mu = 0{\cdot}18$, the phase portrait on plane (x_1, x_2).

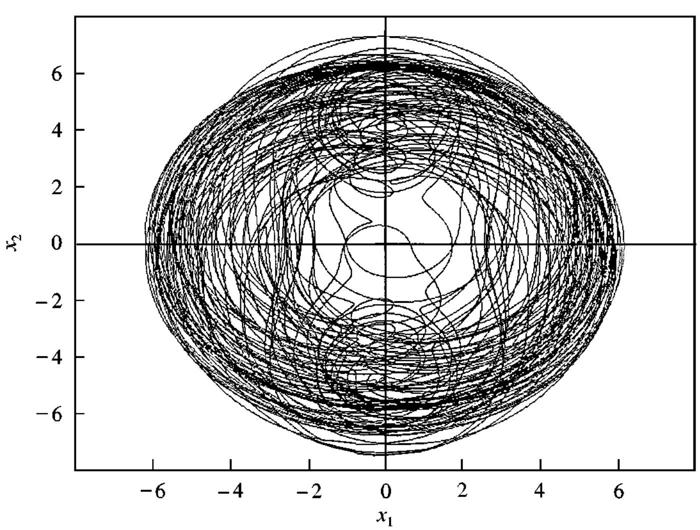

Figure 10. The chaotic response of the averaged equations (28) for $\lambda = 0{\cdot}9$ and $\mu = 0{\cdot}138$, the phase portrait on plane (x_1, x_2).

To show the existence of chaos in the original system (10), the numerical simulations are also performed on the system (10). For the comparison with numerical results obtained above, the two cases are considered. Firstly, the case for $\lambda = b/a = 0{\cdot}7$ is numerically investigated. The other parameters are given as $\alpha_1 = 10{\cdot}3941$, $\beta_1 = 2{\cdot}6082$, $\alpha_2 = \beta_2 = 5{\cdot}9367$, $\omega_1 = \omega_2 = 1$, $\Omega = 2$, and $\varepsilon = 0{\cdot}01$. The chaotic responses of the original system (10) with $\mu = 0{\cdot}16, f_1 = 48{\cdot}8, f_2 = 116{\cdot}963$, and $\mu = 0{\cdot}108$ and $f_2 = 123{\cdot}963$ are given in Figures 11 and 12, respectively, which represent the phase portrait on plane (x_1, x_2). The chosen initial conditions are $x_{10} = -3{\cdot}1$, $x_{20} = 0{\cdot}8$, $x_{30} = 1{\cdot}011$ and $x_{40} = 1{\cdot}4$. The second

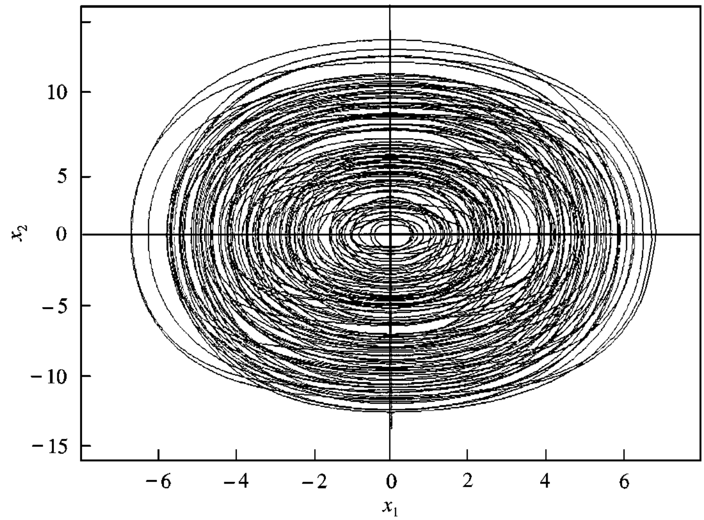

Figure 11. The chaotic response of the original system (10) for $\lambda = 0{\cdot}7$ and $\mu = 0{\cdot}16$, the projection of the phase portrait on plane (x_1, x_2).

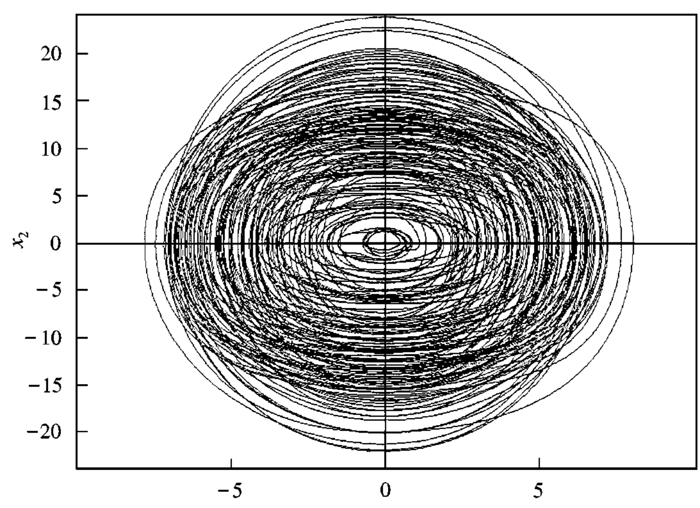

Figure 12. The chaotic response of the original system (10) for $\lambda = 0{\cdot}7$ and $\mu = 0{\cdot}108$, the projection of the phase portrait on plane (x_1, x_2).

case for $\lambda = 0{\cdot}9$ is also studied and the chaotic responses of the original system (10) are given in Figures 13 and 14, where the damped coefficients are $\mu = 0{\cdot}18$ and $0{\cdot}138$ respectively. The chosen parameters and initial conditions are $\alpha_1 = 6{\cdot}3125$, $\beta_1 = 4{\cdot}1778$, $\alpha_2 = \beta_2 = 7{\cdot}3308$, $f_1 = 48{\cdot}8, f_2 = 118{\cdot}963$, $\omega_1 = \omega_2 = 1$, $\Omega = 2$, $\varepsilon = 0{\cdot}01$, $x_{10} = -3{\cdot}1$, $x_{20} = 0{\cdot}8$, $x_{30} = 1{\cdot}011$ and $x_{40} = 1{\cdot}4$.

The numerical results on the averaged equations (28) and the original system (10) illustrate that the chaotic motions in the averaged equations (28) may lead to the amplitude-modulated chaotic oscillations in the original system (10) under the certain

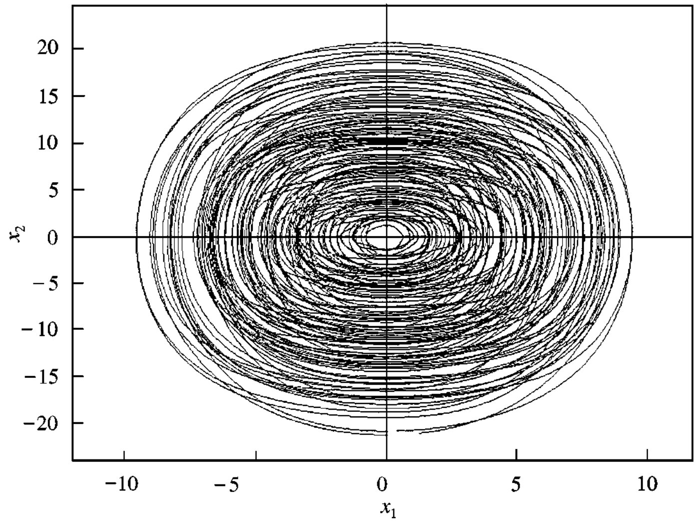

Figure 13. The chaotic response of the original system (10) for $\lambda = 0{\cdot}9$ and $\mu = 0{\cdot}18$, the projection of the phase portrait on plane (x_1, x_2).

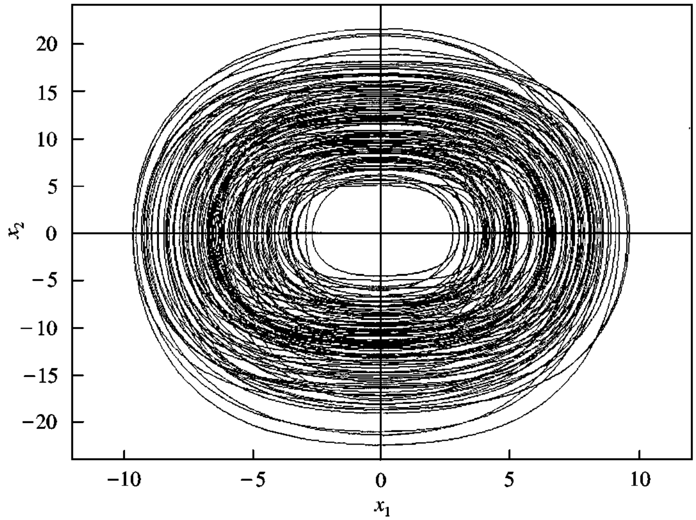

Figure 14. The chaotic response of the original system (10) for $\lambda = 0{\cdot}9$ and $\mu = 0{\cdot}138$, the projection of the phase portrait on plane (x_1, x_2).

conditions. It is seen from the analytical prediction and the numerical simulations given above that the analysis of the averaged equations can indeed predict the chaotic dynamics of the original system qualitatively and quantitatively.

7. CONCLUSIONS

The local and global bifurcations of a rectangular thin plate under parametrical excitation are investigated by the analytical and numerical approaches when the averaged equations have one non-semisimple double zero and a pair of pure imaginary eigenvalues. It is found that the parametrically excited rectangular plate can undergo Hopf bifurcation, heteroclinic bifurcations and Shilnikov-type homoclinic orbit to the saddle focus, which means that there exists the chaotic motion in full four-dimensional system. In order to illustrate the theoretical predictions, the numerical simulation is performed by using Dynamics. The numerical results also show the existence of chaotic motion in the averaged equations. It is well known the chaotic motions in the averaged equations correspond to the amplitude modulated chaotic oscillations in the original system. Therefore, it is demonstrated that there are the amplitude modulated chaotic motions of Silnikov type in parametrically excited rectangular thin plate. It is found from the numerical simulation that the chaotic responses given above are very sensitive to initial conditions.

The case studied in this paper is different from that in references [3,20]. In our investigations, theory of normal form is used to simplify the averaged equations to the normal form. It is noted from the above analysis that based on the normal form, the analysis of global bifurcations and the computation of Melnikov function are simpler than that in references [3, 10, 11, 20]. It is illustrated that the global perturbation method developed by Kovacic and Wiggins [4] may be also applied to the case for the averaged equations being of one non-semisimple double zero and a pair of pure imaginary eigenvalues.

ACKNOWLEDGMENTS

The author gratefully acknowledges the support from the National Natural Science Foundation of China and the Natural Science Foundation of Beijing.

REFERENCES

1. P. J. HOLMES 1981 *Physica D* **2**, 449–481. Center manifolds, normal forms and bifurcations of vector fields with application to coupling between periodic and steady motions.
2. X. L. YANG and P. R. SETHNA 1990 *International Journal of Non-linear Mechanics* **26**, 199–220. Local and global bifurcations in parametrically excited vibrations nearly square plates.
3. Z. C. FENG and P. R. SETHNA 1993 *Nonlinear Dynamics* **4**, 389–408. Global bifurcations in the motion of parametrically excited thin plate.
4. G. KOVACIC and S. WIGGINS 1992 *Physica D* **57**, 185–225. Orbits homoclinic to resonance with an application to chaos in a model of the forced and damped sine-Gordon equation.
5. J. HADIAN and A. H. NAYFEH 1990 *Journal of Sound and Vibration* **142**, 279–292. Modal interaction in circular plates.
6. P. F. PAI and A. H. NAYFEH 1991 *Nonlinear Dynamics* **2**, 445–477. A nonlinear composite plate theory.
7. S. SASSI and G. L. OSTIGUY 1994 *Journal of Sound and Vibration* **178**, 41–54. Effects of initial geometric imperfections on the interaction between forced and parametric vibrations.
8. T. A. NAYFEH and A. F. VAKAKIS 1994 *International Journal of Non-linear Mechanics* **29**, 233–245. Subharmonic travelling waves in a geometrically non-linear circular plate.

9. S. I. CHANG, A. K. BAJAJ and C. M. KROUSGRILL 1993 *Nonlinear Dynamics* **4**, 433–460 Non-linear vibrations and chaos in harmonically excited rectangular plates with one-to-one internal resonance.
10. W. M. TIAN, N. S. NAMACHCHIVAYA and A. K. BAJAJ 1994 *International Journal of Non-linear Mechanics* **29**, 349–366. Non-linear dynamics of a shallow arch under periodic excitation—I. 1 : 2 internal resonance.
11. W. M. TIAN, N. S. NAMACHCHIVAYA and N. MALHOTRA 1994 *International Journal of Non-linear Mechanics* **29**, 367–386. Non-linear dynamics of a shallow arch under periodic excitation—II. 1 : 1 internal resonance.
12. A. ABE, Y. KOBAYASHI and G. YAMADA 1998 *International Journal of Non-linear Mechanics* **33**, 675–690. Two-mode response of simply supported, rectangular laminated plates.
13. A. A. POPOV, J. M. THOMPSON and J. G. CROLL 1998 *Nonlinear Dynamics* **17**, 205–225. Bifurcation analyses in the parametrically excited vibrations of cylindrical panels.
14. N. MALHOTRA and N. SRI NAMACHCHIVAYA 1997 *ASCE Journal of Engineering Mechanics* **123**, 612–619. Chaotic dynamics of shallow arch structures under 1 : 1 internal resonance conditions.
15. N. MALHOTRA and N. SRI NAMACHCHIVAYA 1997 *ASCE Journal of Engineering Mechanics* **123**, 620–627. Chaotic dynamics of shallow arch structures under 1 : 2 internal resonance.
16. C. Y. CHIA 1980 *Non-linear Analysis of Plate*. New York: McMraw-Hill, Inc.
17. A. H. NAYFEH and D. T. MOOK 1979 *Nonlinear Oscillations*. New York: Wiley-Interscience.
18. P. YU, W. ZHANG and Q. BI 2000 *International Journal of Non-linear Mechanics*, Vibration analysis on a thin plate with the aid of computation of normal forms, to appear.
19. S. WIGGINS 1988 *Global Bifurcations and Chaos-Analytical Methods*. New York: Springer-Verlag.
20. Z. C. FENG and S. WIGGINS 1993 *Zeitschriftfuer Angewandte Mathematik und Physikalische* **44**, 201–248. On the existence of chaos in a parametrically forced mechanical systems with broken O(2) symmetry.
21. H. E. NUSSE and J. A. YORKE 1997 *Dynamics*: *Numerical Explorations*. New York: Springer-Verlag.